Available online at www.sciencedirect.com
ScienceDirect
Ceramics International 35 (2009) 2185–2190
CERAMICS INTERNATIONAL
www.elsevier.com/locate/ceramint

Synthesis, characterization and thermal expansion studies on ThO_2–$SmO_{1.5}$ solid solutions

G.G.S. Subramanian, G. Panneerselvam, K.V. Syamala, M.P. Antony *

Fuel Chemistry Division, Indira Gandhi Centre for Atomic Research, Kalpakkam 603 102, India

Received 24 July 2008; received in revised form 15 October 2008; accepted 27 November 2008
Available online 14 January 2009

Abstract

Highly homogeneous $Th_{1-x}Sm_xO_2$; $0 \leq x \leq 0.8$ solid solutions were synthesized by a co-precipitation technique and the co-precipitated samples were sintered at 1473 K. Compositions of the solid solutions were characterized by standard wet-chemical analysis. X-ray diffraction measurements were performed on the sintered pellets for structural analysis, lattice parameter calculation and determination of solid solubility of $SmO_{1.5}$ in ThO_2 matrix. Bulk and theoretical densities of solid solutions were also determined. A fluorite structure was observed for ThO_2–$SmO_{1.5}$ solid solutions with 0–55.2 mol% $SmO_{1.5}$. Thermal expansion coefficients were measured using high temperature X-ray diffraction technique. The mean linear thermal expansivity, $\bar{\alpha}_m$ for ThO_2–$SmO_{1.5}$ solid solutions containing 17.9, 41.7 and 52.0 mol% of $SmO_{1.5}$ were determined in the temperature range 298–2000 K for the first time. The mean linear thermal expansion coefficients for ThO_2–$SmO_{1.5}$ solid solutions are 10.47, 11.16 and 11.45 $\times 10^{-6}$ K^{-1}, respectively.

Keywords: A. Sintering; C. Thermal expansion; E. Nuclear application; B. X-ray methods

1. Introduction

Considering the vast resources of thorium in India and the very limited Indian uranium resources, a study on ThO_2-based fuel and fission product ceramic system(s) is of interest to Indian Nuclear Power [INP] generation program [1,2]. In particular, it is expected that ThO_2 will play an important role as a constituent of nuclear fuel matrix in the third stage of the INP program [3]. Moreover, it is also interesting to note that nuclear scientists and engineers all over the world are engaged in introducing "the thorium fuel cycle" in their respective country's nuclear power program [4–6]. In general, the thorium reserves of the world are estimated to be about three times more than the natural uranium reserves [4].

In view of this, detailed studies on structure and properties of various thoria and related ceramic systems, in particular the solid solutions of fission products in thoria, merit special attention. Rare earth elements, which constitute a major share of the fission products of fuel materials during fuel irradiation, are formed as oxides and get dissolved in the fuel matrix to form solid solutions [7,8]. Synthesis, characterization and estimation of solubility of $LaO_{1.5}$ in ThO_2 and $NdO_{1.5}$ in ThO_2 were carried out in our previous work [9,10]. We have also determined thermal expansion characteristics of the solid solutions containing different mol% of $LaO_{1.5}$ and $NdO_{1.5}$ in ThO_2 [11,12].

Samarium oxide is considered a good representative candidate of ThO_2—rare earth oxide solid solution family [13]. ThO_2 can dissolve considerable amounts of samarium oxide in its fluorite lattice [14,19]. However, not much data are available in open literature on the thermal expansion characteristics of ThO_2–$SmO_{1.5}$ solid solutions.

In this context, we have been investigating various thorium-based mixed oxide systems. One of the major activities is on the studies of thermal expansion behaviour of different thoria-based systems having relevance to the proposed thorium oxide-based nuclear reactors. An attempt has been made to measure the lattice thermal expansion of ThO_2–$SmO_{1.5}$ solid solutions by high temperature X-ray powder diffraction technique.

2. Experimental details

2.1. Sample preparation

Nuclear grade thorium nitrate $Th(NO_3)_4{\cdot}5H_2O$ (99.97% pure) and samarium oxide (99.97% pure) used in the present

* Corresponding author. Tel.: +91 4114 27480098; fax: +91 4114 27480065.
E-mail address: mpa@igcar.gov.in (M.P. Antony).

0272-8842/$34.00
doi:10.1016/j.ceramint.2008.11.020

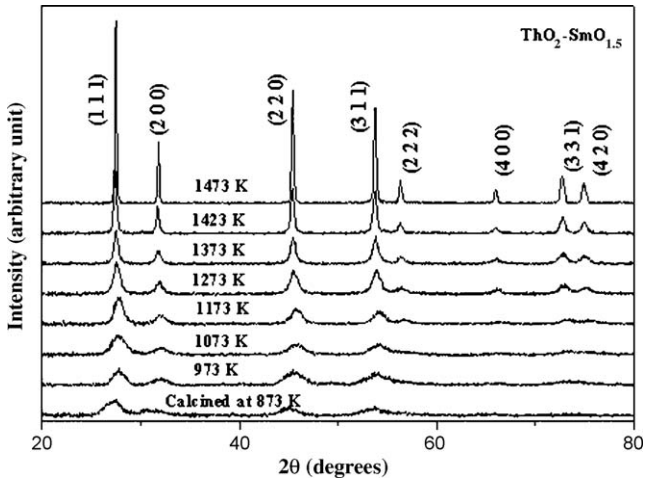

Fig. 1. Evolution of powder patterns as the function of sintering temperature are graphically illustrated.

work were obtained from M/s. Indian Rare Earths Ltd. Chemical analysis of thorium nitrate and samarium oxide has been carried out using ICPMS (Inductively Coupled Plasma Mass Spectrometer) to confirm the purity. The preparation methodology is briefly illustrated in our earlier paper [9]. The XRD patterns were recorded for the sintered pellet to confirm the successful formation of solid solution is presented in Fig. 1. It was found that sintering at 1473 K for about 6 h resulted in fairly dense (~94% of theoretical density) ceramic compacts.

2.2. Characterization

For the compositional characterization of ThO_2–$SmO_{1.5}$ solid solutions, a known amount (0.5–1 g) of the sample was dissolved in hot concentrated nitric acid in presence of traces of HF. The analysis for thorium and samarium were carried out by successive titration with DTPA (Diethylene Triamine Penta Acetic acid) under controlled pH condition [20].

The bulk density measurement of the solid solutions was made by standard liquid immersion technique employing dibutyl phthalate as the immersing liquid. The theoretical density (X-ray density) was estimated from the lattice parameter data obtained by XRD experiments.

The lattice parameter measurements were carried out by X-ray diffraction. The X-ray studies were carried out in a Philips X'Pert MPD® system with Cu Kα radiation in Bragg-Brentano geometry. The XRD data were obtained in the 2θ range varying from 20° to 80° with an interval of 0.02°. An effective high angle corrected lattice parameter for each composition was determined using Nelson–Riley interpolation scheme [21]. The accuracy of the measurement of lattice parameter is about ±0.001 nm.

2.3. Thermal expansion studies

The thermal expansion characteristics of the solid solutions were studied from room temperature to 2000 K using HT-XRD. The HT-XRD studies were performed in a Philips-X'pert MPD® system, equipped with the Bühler® high vacuum heating stage. Typical instrument related parameters were: operating voltage of 40 kV; current of 30 mA for the X-ray tube; scan speed of 0.02° s^{-1} with a counting time of 6 s per step and an angular range (2θ) of 20–80°. The heating stage consisted of a thin (~80 μm) resistance heated tantalum foil, on top of which the sample was placed. The temperature was measured by a W-Re thermocouple, which was spot-welded to the bottom of the tantalum heater. The temperature was controlled to an accuracy of about ±1 K. The diffraction studies were performed using Cu Kα radiation in the Bragg-Brentano geometry, at a temperature interval of 50 K up to 2000 K. A heating rate of 1 K min^{-1} and a holding time of 60 min at each temperature of measurement were adopted. The specimen stage was flushed with high purity argon before the start of every experimental run and a vacuum level of about 10^{-5} mbar was maintained throughout the experiment. Acquisition and preliminary analysis of data were performed by the Philips X'pert Pro® software, although at a latter stage, we resorted to an independent processing of the raw data for a precise determination of the peak position.

3. Results and discussion

3.1. Solubility limit

In Table 1, the density *versus* composition data as determined from immersion and XRD techniques are listed. As may be seen, the X-ray density is always higher than the corresponding bulk density, attesting to the presence of porosity in the sintered samples. However, it is gratifying to note that without the addition of any binder and besides adopting relatively a low-temperature sintering procedure, we could achieve about 93% of theoretical density. This advantage derives from the enhanced homogeneity of the initial powder mix obtained from the co-precipitation technique [22].

In Fig. 2, a collage of X-ray diffraction patterns obtained for various $Th_{1-x}Sm_xO_2$ compositions is presented. With increasing concentration of $SmO_{1.5}$ in the solid solution, the various

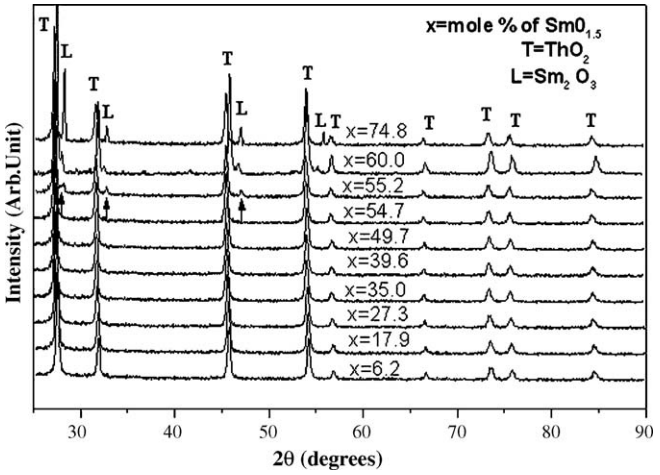

Fig. 2. The X-ray diffraction profiles (Cu Kα radiation) obtained for various concentrations of Sm_2O_3 in ThO_2 are presented as a collage.

Table 1
Listing of composition, lattice parameter, bulk and theoretical densities of $Th_{1-x}Sm_xO_2$ system.

Solid solution no.	Mole fraction of $SmO_{1.5}$	Lattice parameter (nm)	Bulk density (10^{-3} kg m^{-3})	X-ray density (10^{-3} kg m^{-3})	Percentage theoretical density
1	6.2	0.5600	9.11	9.79	93.0
2	12.3	0.5608	8.93	9.56	93.4
3	17.9	0.5614	8.77	9.36	93.7
4	22.8	0.5621	8.62	9.17	94.0
5	27.3	0.5629	8.49	9.00	94.4
6	31.5	0.5633	8.37	8.86	94.5
7	35.0	0.5635	8.27	8.74	94.6
8	39.6	0.5643	8.13	8.56	95.0
9	41.7	0.5646	8.05	8.49	94.9
10	44.7	0.5649	7.99	8.38	95.3
11	47.0	0.5653	7.91	8.29	95.3
12	48.6	0.5654	7.82	8.24	94.9
13	49.1	0.5656	7.85	8.24	95.3
14	49.7	0.5656	7.80	8.20	95.1
15	51.1	0.5658	7.73	8.15	94.8
16	52.0	0.5659	7.64	8.12	94.1
17	53.4	0.5661	7.67	8.07	95.1
18	54.7	0.5662	7.62	8.02	95.0
19	55.2	0.5663	7.58	8.01	94.7
20	60.0	0.5663	7.49	7.86	95.3
21	64.7	0.5663	7.29	7.72	94.5
22	70.2	0.5663	7.21	7.56	95.5
23	74.8	0.5663	7.10	7.42	95.7
24	79.7	0.5663	6.99	7.27	96.1
25	84.9	0.5663	6.90	7.12	97.0
ThO_2	Pure	0.5597	9.70	10.00	–
Sm_2O_3	Pure	1.09290	6.776	7.069	–

peak positions reveal a mild shift towards the lower angle side. This is consistent with the overall increase in lattice parameter that ensues upon the addition of samaria to thoria. Further, this point is also corroborated by the bulk density data, in that there is a gradual decrease in density with increasing mole fraction of $SmO_{1.5}$. This is illustrated in Fig. 3. In Fig. 3, the composition dependence of lattice parameter is also graphically displayed. It emerges from Fig. 3 that the steady increase in lattice parameter with respect to the addition of samaria reaches a maximum, at about 55 mol%; after which an almost constant behavior is noticed. The onset of this solubility limit is also clearly reflected in the corresponding XRD profiles (Fig. 2). It is instructive to note from Fig. 2, that up to about 54.7 mol% of $SmO_{1.5}$ in ThO_2, the XRD profiles are qualitatively similar. But upon reaching the solubility limit say, about 55.2 mol%, small, yet distinctly visible humps are noticed in the XRD profile. These are marked by small arrow marks in Fig. 2. With further additions of $SmO_{1.5}$, these humps begin to manifest as distinct peaks, which are characteristic of Sm_2O_3 (Fig. 2). This suggests that for $SmO_{1.5}$ concentrations higher than about 55.4 mol%, the limit of solubility has already been reached and an entry in to the two-phase field has been made. Combining this information and the lattice parameter variation as given in Fig. 3, we conclude that within the resolution limit set by our experimental techniques, the maximum solubility of $SmO_{1.5}$ in ThO_2 from room temperature to 1473 K is in the range 54.7–55.2 mol% via co-precipitation route.

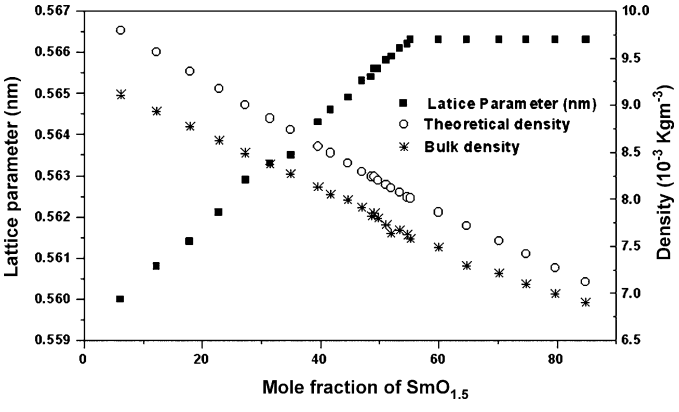

Fig. 3. Composition dependence of lattice parameter and density in $Th_{1-x}Sm_xO_2$ system is graphically illustrated.

The solubility limit estimated in the present study is compared with the previously reported values [14–19]. The details regarding the solubility limits of various rare earth oxides in ThO_2 as obtained by different workers are listed in our previous paper [9]. Sibieude and Foex [15] prepared thoria—rare earth oxide phases and determined the phase transitions from room temperature to its melting point and they found 50 mol% $SmO_{1.5}$ is soluble in thoria at 1673 K. Comparing our results with that of Sibieude and Foex [15], it may be seen that the presently reported solubility limit is 5% higher than that reported by Sibieude and Foex. Also, it must be noted that this higher solubility was achieved at relatively lower temperature. This may be due to the difference in the method of preparations

of solid solutions. Sibieude and Foex adopted a solid-state route where as the present study adopted the wet-chemical method, which ensures better chemical homogeneity. In addition Keller studied the solubility of $SmO_{1.5}$ in ThO_2 up to 39.5 mol% at 1573 K [14].

Thoria belongs to cubic CaF_2 structure, where as $SmO_{1.5}$ adopts BCC (Mn_2O_3-type) structure [23]. Apart from this, the ionic radius of thorium atom (1.02 Å) is slightly smaller than samarium (1.08 Å) in eightfold co-ordination arrangement and valency of the thorium is +4 whereas that of samarium is +3 [24]. Therefore 100% solid solubility between thoria-samarium oxide systems is not possible. Hence, addition of samarium into thorium sublattice introduces considerable lattice strain that is reflected in the increasing lattice parameter trend. In addition, it also entails that with the replacement of each thorium atom in its sublattice by samarium, the oxygen stoichiometry of the ThO_2 lattice is considerably affected. In fact, the oxygen deficiency following samaria addition is accommodated through the formation of charge compensated defect structures [18]. Thus, an overall alteration, probably a reduction in the net attractive electrostatic contribution to the structural stability ensues as a natural consequence of ThO_2–$SmO_{1.5}$ solid solution formation. It must be noted that there are two factors, which seem to control lattice parameters in this type of systems. One is the smaller size of Th^{4+} as compared to Sm^{3+} ion, which should increase the lattice parameter and second is the introduction of extra-interstitial oxygen ions, which are expected to cause repulsion and increase the lattice parameter. On increasing Sm^{3+} content, in ThO_2–$SmO_{1.5}$ series, it seems that the former factor predominates over the latter [25].

3.2. Thermal expansion studies

The lattice parameter (a) in each case was estimated by considering the eight major reflections of the CaF_2 structure. Fig. 4 shows the effective lattice parameter thus obtained as a function of temperature.

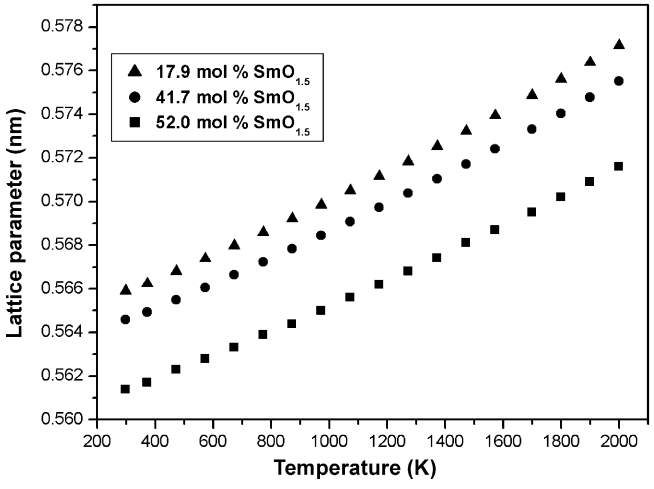

Fig. 4. The temperature variation of corrected lattice parameter of ThO_2–$SmO_{1.5}$ solid solutions is illustrated.

For the purpose of calculating thermal expansivity, the corrected lattice parameter data with temperature (K) are fitted to a second-degree polynomial in the temperature increment $(T - 298)$. The variation of lattice parameter, a, with the temperature in this study is given by the following equations:

For ThO_2–17.9 mol% samarium oxide solid solution,

$$a_T(\text{nm}) = 0.5599 + 4.6032 \times 10^{-6}(T - 298) + 6.0813 \times 10^{-10}(T - 298)^2 \quad (1)$$

For ThO_2–41.7 mol% samarium oxide solid solution,

$$a_T(\text{nm}) = 0.56304 + 4.9042 \times 10^{-6}(T - 298) + 6.7293 \times 10^{-10}(T - 298)^2 \quad (2)$$

For ThO_2–52.0 mol% samarium oxide solid solution,

$$a_T(\text{nm}) = 0.56304 + 5.0329 \times 10^{-6}(T - 298) + 7.0197 \times 10^{-10}(T - 298)^2 \quad (3)$$

where T is in Kelvin. The above equations are valid in the temperature range 298–2000 K. Once the lattice parameter is known as a function of temperature, it is possible to estimate the instantaneous (α_L-instantaneous), mean (α_L-mean) linear thermal expansion coefficients and expansion % by the following relations:

$$\alpha_L\text{-instantaneous} = \left(\frac{1}{a_T}\right)\left(\frac{da_T}{dT}\right). \quad (4)$$

$$\alpha_L\text{-mean} = \left(\frac{1}{a_{298}}\right) \times \left\{\frac{a_T - a_{298}}{T - 298)}\right\}. \quad (5)$$

$$\text{Expansion}\,(\%) = 100 \times \left\{\frac{a_T - a_{298}}{a_{298}}\right\}. \quad (6)$$

In the above expression, a_T represents the lattice parameter at temperature T and a_{298} the corresponding value at 298 K. The percentage linear thermal expansions of the solid solutions were computed using Eq. (6). The computed data of percentage thermal expansion as a function of temperature, instantaneous (αi) and mean (αm) linear thermal expansivities are presented in Table 2.

It must be mentioned that to the best of our knowledge, no HT-XRD-based lattice thermal expansion data for ThO_2–$SmO_{1.5}$ solid solutions are available in the open literature. The room temperature lattice parameter values estimated in the present study for the ThO_2–$SmO_{1.5}$ solid solutions containing 17.9, 41.7 and 52.0 mol% $SmO_{1.5}$ were found to be 0.5614, 0.5646 and 0.5659 nm. From Fig. 4, it is observed that the lattice parameter of all the solid solutions increases progressively with increasing temperature. In Fig. 5, we present the percentage linear thermal expansion estimated for these solid solutions. For the sake of comparison, we also present in Fig. 5, the mean thermal expansion % value for pure thoria [26] taken from the literature. The percentage thermal expansion of solid solutions and thoria increase with increasing temperature as expected.

Table 2
HT-XRD data on ThO_2–$SmO_{1.5}$ solid solution.

T (K)	17.9 mol% $SmO_{1.5}$			41.7 mol% $SmO_{1.5}$			52 mol% $SmO_{1.5}$		
	TE (%)	αi (10^{-6} K^{-1})	αm (10^{-6} K^{-1})	TE (%)	αi (10^{-6} K^{-1})	αm (10^{-6} K^{-1})	TE (%)	αi (10^{-6} K^{-1})	αm (10^{-6} K^{-1})
298	0.000	8.26	–	0.000	9.40	–	0.000	9.63	–
373	0.061	8.41	8.08	0.060	9.58	8.02	0.059	9.82	7.88
473	0.153	8.60	8.74	0.158	9.81	8.99	0.160	10.07	9.11
573	0.248	8.80	8.98	0.258	10.05	9.36	0.263	10.32	9.52
673	0.343	8.99	9.12	0.360	10.29	9.58	0.368	10.56	9.78
773	0.441	9.19	9.24	0.465	10.53	9.75	0.476	10.81	9.96
873	0.541	9.38	9.36	0.572	10.77	9.89	0.585	11.06	10.12
973	0.643	9.57	9.47	0.682	11.01	10.03	0.698	11.31	10.27
1073	0.747	9.76	9.57	0.793	11.24	10.15	0.813	11.56	10.40
1173	0.853	9.95	9.67	0.907	11.48	10.27	0.929	11.80	10.52
1273	0.962	10.15	9.77	1.023	11.72	10.39	1.049	12.05	10.65
1373	1.072	10.34	9.87	1.141	11.96	10.50	1.171	12.30	10.77
1473	1.185	10.52	9.97	1.262	12.20	10.61	1.295	12.55	10.88
1573	1.301	10.71	10.07	1.385	12.44	10.71	1.422	12.80	10.99
1700	1.450	10.95	10.19	1.544	12.74	10.85	1.585	13.11	11.13
1800	1.569	11.14	10.29	1.673	12.98	10.95	1.718	13.36	11.24
1900	1.691	11.33	10.38	1.803	13.22	11.06	1.852	13.61	11.35
2000	1.815	11.51	10.47	1.936	13.45	11.16	1.988	13.86	11.45

Percentage thermal expansion as a function of temperature, instantaneous (αi) and mean (αm) linear thermal expansivities La_2O_3.

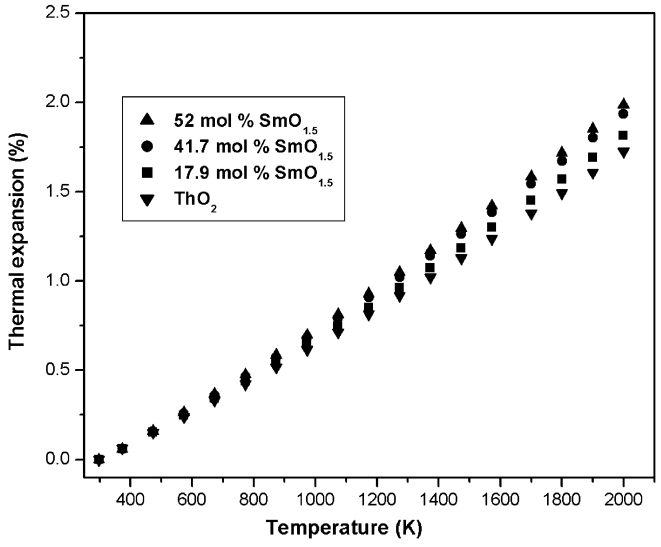

Fig. 5. The percentage linear thermal expansion estimated from the lattice parameter of ThO_2–$SmO_{1.5}$ solid solutions are plotted together with the corresponding data on pure ThO_2.

4. Conclusions

A series of solid solutions containing $SmO_{1.5}$ in ThO_2 were prepared by the co-precipitation method. Composition, structure and density of the solid solutions were characterized. There are two distinct regions in the systems viz. a solid solution of $SmO_{1.5}$ in ThO_2, which are identified as a cubic fluorite, and a biphasic region of ThO_2 type and $SmO_{1.5}$ type phases. The solubility limit of $SmO_{1.5}$ in ThO_2 at 1473 K has been determined by X-ray diffraction. The percent linear thermal expansion in this temperature range, for ThO_2–$SmO_{1.5}$ solid solutions containing 17.9, 41.7 and 52.0 mol% $SmO_{1.5}$ are 1.82, 1.94 and 1.99, respectively. It is suggested that the solid solutions are stable up to 2000 K. It is also suggested that the effect and nature of the dopant are the important parameters influencing the thermal expansion of ThO_2.

Acknowledgements

The authors are grateful to Dr. Baldev Raj, Dr. P.R. Vasudeva Rao and Dr. T.G. Srinivasan for their keen interest and encouragement during the course of this work.

References

[1] K. Sreenivas Rao, P.V. Achuthan, C.V. Narayanan, A. Ramanujam, V.P. Kansra, K. Balu, in: Proceedings of Conference on Power from Thorium: Status, Strategies and Directions (INSAC-2000), Vol. 1, Mumbai, India, (2000), p. 157.
[2] K. Anantharaman, A. Ramanujam, H.S. Kamath, S. Majumdar, V.N. Vaidya, M. Venkataraman, in: Proceedings of Conference on Power from Thorium: Status, Strategies and Directions (INSAC-2000), Vol. 2, Mumbai, India, (2000), p. 107.
[3] R. Chidambaram, M. Srinivasan, I. Kimura (Eds.), Proceedings of the ISmO-Japan Seminar on Thorium UtilizationBombay, Indian Nuclear society and Atomic Energy Society of Japan, December, Bombay, India, (1990), p. 7.
[4] R.D. Nininger, Minerals for Atomic Energy, D. Van Nostrand, New York, 1955, p. 16.
[5] P.G. Boczar, G.R. Dyck, J.D. Sullivan, R.J. Ellis, R.T. Jones, P. Taylor, A fresh look at thorium fuel cycles in CANDU reactors, Paper presented at IAEA Advisory Group Meeting on Thorium Fuel Cycle Perspectives, 1997.
[6] H.T. Akie, T. Muromura, H. Takano, S. Matsuura, Nucl. Technol. 107 (1994) 182.
[7] D.R. Olander, Fundamental Aspects of Nucl Reactor Fuel Elements, NTIS, Springfield, 1976.
[8] C.E. Johnson, I. Johnson, P.E. Blackburn, C.E. Crouthamel, Reactor Technol. 15 (1972/73) 303.

[9] G. Panneerselvam, M.P. Antony, T. Vasudevan, Mater. Lett. 58 (25 (October)) (2004) 3192–3196.
[10] G. Panneerselvam, M.P. Antony, P.R. Vasudeva Rao, Trans. The Indian Ceram. Soc. 65 (2) (2006).
[11] G. Panneerselvam, M.P. Antony, T. Vasudevan, J. Alloys Compd. 415 (1–2 (18 May)) (2006) 26–30.
[12] G. Panneerselvam, M.P. Antony, T. Vasudevan, Thermochim. Acta 443 (1 (1 April)) (2006) 109–115.
[13] C.A. Alexander, et al., Fission Product Transport in Reactor Accidents, Hemisphere, New York, 1990, p. 127.
[14] C. Keller, U. Berndt, H. Engerer, L. Leitner, J. Solid State Chem. 4 (1972) 453.
[15] F. Sibieude, M. Foex, J. Nucl. Mater. 56 (1975) 229.
[16] A.M. Diness, R. Roy, J. Mater. Sci. 4 (1969) 613.
[17] P. Srirama Murti, C.K. Mathews, J. Phys. D: Appl. Phys. 24 (1991) 2202.
[18] I.G. Brauer, H. Gradinger, Z. Anorg. Chem. 276 (1954) 209, as cited in Ref. [8].
[19] R.S. Roth, T. Negas, L.P. Cook, Phase Diagram for Ceramists, vol. 4, NBS Compilation, p. 132.
[20] R. Pribil, V. Vesely, Talanta 10 (1963) 899.
[21] B.D. Cullity, Elements of X-ray Diffraction, 2nd edition, Addison-Wesely Co., Reading, MA, 1978, Chapter 11.
[22] G.D. White, L.A. Bray, P.E. Hart, J. Nucl. Mater. 96 (1981) 305.
[23] E.C. Subbarao, P.H. Sutter, J. Hrizo, J. Am. Ceram. Soc. 48 (1965) 443.
[24] R.D. Shannon, Acta Crystallogr. A 31 (1976) 751.
[25] B.P. Mandal, V. Grover, A.K. Tyagi, Mater. Sci. Eng. A 430 (2006) 120–124.
[26] J. Belle, R.M. Berman, Thorium dioxide: Properties and Nuclear Applications DOE/NE-0060, 1984.R.